Advanced Pharmaceutical Bulletin, **2013**, 3(1), 189-195
doi: http://dx.doi.org/10.5681/apb.2013.031
http://apb.tbzmed.ac.ir/

Targeted Fluoromagnetic Nanoparticles for Imaging of Breast Cancer MCF-7 Cells

Mostafa Heidari Majd[1,2,3], Jaleh Barar[1,4]*, Davoud Asgari[1], Hadi Valizadeh[1], Mohammad Reza Rashidi[1], Vala Kafil[1], Javid Shahbazi[1], Yadollah Omidi[1,4]

[1] *Research Center for Pharmaceutical Nanotechnology, Faculty of Pharmacy, Tabriz University of Medical Sciences, Tabriz, Iran.*
[2] *Faculty of Pharmacy, Zabol University of Medical Sciences, Zabol, Iran.*
[3] *Student Research Committee, Tabriz University of Medical Sciences, Tabriz, Iran.*
[4] *Ovarian Cancer Research Center, University of Pennsylvania, Philadelphia, USA.*

ARTICLEINFO

Article Type:
Research Article

Article History:
Received: 25 October 2012
Revised: 26 November 2012
Accepted: 26 November 2012
ePublished: 7 February 2013

Keywords:
Magnetic nanoparticles
Folate receptor
Breast cancer
MCF-7 cells
Internalization

ABSTRACT

Purpose: To achieve simultaneous imaging and therapy potentials, targeted fluoromagnetic nanoparticles were synthesized and examined in human breast cancer MCF-7 cells. ***Methods:*** Fe_3O_4 nanoparticles (NPs) were synthesized through thermal decomposition of $Fe(acac)_3$. Then, magnetic nanoparticles (MNPs) modified by dopamine-poly ethylene glycol (PEG)-NH_2; finally, half equivalent fluorescein isothiocyanate (FITC) and half equivalent folic acid were conjugated to one equivalent of it. The presence of Fe_3O_4-DPA-PEG-FA/FITC in the folate receptor (FR) positive MCF-7 cells was determined via fluorescent microscopy to monitor the cellular interaction of MNPs. ***Results:*** FT-IR spectra of final compound confirmed existence of fluorescein on folic acid grafted MNPs. The Fe_3O_4-DPA-PEG-FA/FITC NPs, which displayed a size rang about 30-35 nm using scanning electron microscopy (SEM) and transmission electron microscopy (TEM), were able to actively recognize the FR-positive MCF-7 cells, but not the FR-negative A549 cells. ***Conclusion:*** The uniform nano-sized Fe_3O_4-DPA-PEG-FA/FITC NPs displayed great potential as theranostics and can be used for targeted imaging of various tumors that overexpress FR.

Introduction

While smart multifunctional nanomedicines and theranostics are becoming robust seamless tools for simultaneous imaging and therapy of cancer, for their effective clinical implementations we need a) to advance technologies for specific targeting of cancer cells, b) to improve imaging/sensing methods, c) to develop biocompatible long circulating bioshuttles for simultaneous delivery of targeting moiety, imaging agent and therapy, and d) to track and control cancerous single cells/bioconvoys to avoid distribution of oncogenic messages, the so called metastasis.[1] Of various advancements holding great promise for improving the sensing/imagining cancerous cells, superparamagnetic/magnetic NPs as effective contrast agents,[2-4] appear to meet such criteria.

MNPs have been used as nanocarriers for specific delivery of chemotherapy agents.[5-7] Possessing unique properties, they can be conjugated with different moieties such as targeting and therapeutics agents. Also MNPs have been used for various purposes such as magnetic bio separation, cell labeling, hyperthermia treatment of solid tumors and contrast agents for magnetic resonance imaging (MRI).[8-10]

In biological micro-compartments such as tumor microenvironment, the surface-modified MNPs ensue to display excellent dispersion characteristics, while the unmodified MNPs have high propensity to form agglomerated macrostructures that can be taken up by mononuclear phagocyte system (MPS) resulting in significant loss of MNPs in blood circulation.[11,12] Surface modification of MNPs with biocompatible polymers (e.g., polyethylene glycol (PEG)) can markedly protect them against immune system clearance providing longer circulation in blood. Further, surface modifications of MNPs were shown to improve their stability, biocompatibility, drug loading potential, and interaction capability with the target cells/tissues.[13,14] MNPs can become stealth through PEGylation, at which they can circumvent the opsonization.[15,16] PEG grafts also provide further conjugation potential with homing devices while keeping them longer in the blood stream and thus providing higher accumulation in the target sites.[11]

Targeted MNPs are often armed with moieties that enable them to detect the disease specific markers such as cancer marker molecules (CMMs), resulting in simultaneous targeted therapy and imaging. Of CMMs, folate receptors were shown to be upregulated in various tumors[17] thus can be targeted by folic acid (FA) which displays extremely high affinity to the folate

***Corresponding author:** Jaleh Barar, Ovarian Cancer Research Center, University of Pennsylvania, Philadelphia, USA.
Email: jbarar@mail.med.upenn.edu

receptors. Previously, we have capitalized on synthesis of targeted fluorophoromagnetic nanoparticles conjugated with mitoxantrone (MTX).[18] To pursue the internalization of the FA conjugated MNPs by the FR positive breast cancer MCF-7cells, in the current study, we exploited FA conjugated PEGylated MNPs labeled with Fluorescein isothiocyanate (FITC). Conjugation of FA to the surface of MNPs can combine the passive targeting potential of MNPs with active targeting capabilities, resulting in enhanced permeation and retention (EPR) effects together with increased specific targeting of the tumor cells.[16,19] FITC has widely been used for optical detection of NPs by fluorescence microscopy and flow cytometry, so we functionalized MNPs with an isothiocyanate through reactive group (-N=C=S) that can react with terminal amines.[20]

Materials and Methods

Iron (III) acetylacetonate ($Fe(acac)_3$) and benzyl ether were purchased from Merck chemical company (Hohenbrunn, Germany). Poly Ethylene Glycol (PEG_{2000}), triethylamine, N,N, dicyclohexyl-carbodiimide (DCC), and N-hydroxysuccinimide (NHS) were purchased from Merck Chemical Company (Darmstadt, Germany). Oleylamine, bromoacetyl chloride, fluorescein isothiocyanate isomer I (FITC), RPMI 1640 media, MTT and dopamine hydrobromide (DPA) were purchased from Sigma-Aldrich Company (Steinheim, Germany). Folic acid was purchased from Acros Organics Company (New Jersey, USA). N-tert-Butoxycarbonyl-1, 2-ethylenediamine was purchased from Alfa Aesar Company (Lancashire, UK). Penicillin-Streptomycin and Fetal Bovine Serum were purchased from Invitrogen (Paisley, UK). MCF-7 cell lines were purchased from Pastor Cell bank (Iran). All other reagents and solvents were common analytical grade and pure.

Preparation of Fe_3O_4 Nanoparticles

$Fe(acac)_3$(2.12 g, 6.0 mmol) was dissolved in a mixture of benzyl ether and oleylamine (30 mL: 30 mL) and were stirred by magnetic stirrer.[21-23] The solution was dehydrated at 120 °C for 1h using Dean-Stark apparatus and under flow of argon. After 1 h, temperature was raised quickly to 270 °C for 2 h under argon. The reaction mixture was cooled down to room temperature and then ethanol (80 mL) was added to the dark brown mixture and precipitated with centrifuge at 5000 rpm. The product was re-dispersed in 30 mL n-hexane and stored at 4 °C.[18] Figure 1 Step 1 represents this process. The yield was 1.8 g, i.e. 84.9%.

Synthesis of O-(2'-Boc-Imino-Ethylene-Imino)-O'-(2-Dopamineacetyl) Polyethylene Glycol (DPA-PEG-NHBoc)

For synthesise of DPA-PEG-NHBoc, we conducted three main steps as described previously.[22]

First, polyethylene glycol (PEG_{2000}) (10.0 g, 5.0 mmol), bromoacethyl chloride (1.75 mL, 20.0 mmol) and triethylamine (2.8 mL, 20 mmol) were dissolved in 20 mL dichloromethane. H-NMR result was: δH (400 MHz; $CDCl_3$) 3.55-3.70 (234 H, -O-CH_2-CH_2-O-), 4.07 (4H, s, –CH_2-Br) and 4.32 (4H, t, –CH_2-COO-).

Second, BBrAC-PEG (7.50 g, 3.345 mmol) was dissolved in 250 mL dichloromethane, then dopamine hydrobromide (0.817 g, 3.487 mmol), KI (0.277 g, 1.6725mmol) and K_2CO_3 (1.615g, 11.707mmol) were added to the solution. H-NMR result was: δ H(400 MHz; $CDCl_3$) 2.69 (2H, t, -CH_2-CH_2N-), 2.90 (2H, t, –Ph-CH_2-CH_2-), 3.5-3.7 (234 H, -O-CH_2-CH_2-O-), 4.0979 (2H, s, –CH_2-Br), 4.245 (4H, t, –CH_2-COO-), 6.54 (1H, d, Ph) and 6.74 (2H, m, Ph).

Third, DPA-PEG-BrAC (6.00 g, 2.51mmol) and N-tert-butoxycarbonyl-1,2-ethylenediamine (0.475g, 3.012mmol) were dissolved in dichloromethane (250 mL). Then, KI (0.50 g, 3.012mmol) and K_2CO_3 (1.757 g, 12.552 mmol) were added. H-NMR result was: δ H(400 MHz; $CDCl_3$) 1.409 (9H, s, t-Bu), 2.66 (2H, t, –CH_2-CH_2N-), 2.80 (2H, t, –Ph-CH_2-CH_2), 2.90 (2H, t, –CH_2-CH_2-NHBoc), 3.22 (2H, t, -CH_2-NHBoc), 3.5-3.7 (234 H, -O-CH_2-CH_2-O-), 4.1 (2H, s, Ph-CH_2-CH_2-NH-CH_2- and 2H of –CH_2-NH-CH_2-CH_2- NHBoc), 4.33 (4H, t, - CH_2-COO-), 6.53 (1H, d, Ph) and 6.76 (2H, m, Ph).

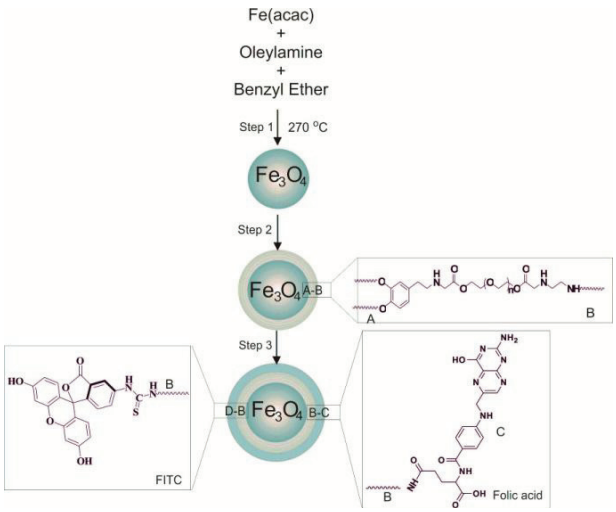

Figure 1. Schematic representation of step-wise synthesis of Fe_3O_4-DPA-PEG-FA/FITC nanoparticles.

All The solutions were stirred overnight under argon at room temperature (RT) also the insoluble compounds filtered using Buchner vacuum filtration funnel. In three steps for purification of the products, the solvent (dichloromethane) was removed using a rotary vacuum evaporator (Heidolph, Schwabach, Germany) and 30 mL diethyl ether was added for precipitation. Diethyl ether was removed using a rotary evaporator, and then products were redissolved in water/NaCl (35%w/v). Products were extracted from water by the addition of 30 mL dichloromethane and re-precipitation with 30 mL diethyl ether.

DPA-PEG-NHBoc (1.0 g, 0.04 mmol) was dissolved in dichloromethane (20 mL). The solution was stirred using a magnetic stirrer. Then trifluoroacetic acid (1.5 mL) was added and stirred for 1h at RT. Solvent was removed by rotary and product (DPA-PEG-NH_2) was washed (3×) with dichloromethane. The final brown color product was precipitated using diethyl ether.

Preparation of Fe_3O_4-DPA-PEG-NH_2 and Conjugation

Fe_3O_4 (0.5 g, 2.16 mmol) was dispersed in dichloromethane (50 mL).[22] DPA-PEG-NH_2 (2.5 g) was added to the solution and stirred overnight under argon blanket at 25 °C. After one night, solutions were sonicated for 15 min and then, Fe_3O_4-DPA-PEG-NH_2 was precipitated using hexane and gathered by centrifugation at 4000 rpm. For purification of modified Fe_3O_4, the samples were washed (3×) with dichloromethane/hexane (1:5) mixture. Finally, the solid dark-brown color product was re-dispersed in 20 mL ethanol. Figure 1 schematically represents the engineering process.

For conjugation, in the first step, N,N,dicyclohexylcarbodiimide (DCC) (2.95 g, 14.3 mmol), folic acid (3g, 6.8 mmol) and N-hydroxysuccinimide (NHS) (1.643 g, 14.3 mmol) were dissolved in dimethylsulfoxide (DMSO) (30 mL) (2.1:1:2.1mmol).[24] Triethylamine (1.88 mL, 13.6 mmol) was added to the solution while solution was stirred overnight at RT under argon blanket. Then, hexane (40 mL) was added to the flask for precipitation and yellow color product was washed with ether (yield was 1.66 g, 55.33%).

In the second step, modified Fe_3O_4-DPA-PEG-NH_2 (1.00 g) was dispersed in 10 mL DMSO, and then triethylamine (0.17 mL, 1.248 mmol) was added to the solution.[25] FA-NHS (0.0985 g, 0.156 mmol) and fluorescein isothiocyanate (FITC) (0.0607 g, 0.156 mmol) were each dissolved in DMSO (5 mL). The two solutions were added to the reaction flask containing compound and stirred at room temperature overnight under argon blanket. The final product was collected with Invitrogen bead separation system (DYNAL), washed with deionized water (3×) and characterized by FT-IR (Shimadzu FT-IR-8400S spectrophotometer, Shimadzu Scientific Instruments, Japan).

Cell Culture

The FR-positive MCF-7 cell line and the FR-negative lung cancer cell line were used for this study. Both cell lines were cultured at a seeding density of 4.0 × 10^4cells/cm^2 onto the cultivation plates/coverslips using normal culture medium (DMEM supplemented with 10% FBS, 100 units/mL penicillin G and 100 µg/mL streptomycin). The cultured cells were kept at 37 °C in a humidified CO2 incubator during cultivation and during experiments.

Fluorescence Microscopy

For fluorescence microscopy, cells were cultivated as described onto the 22-mm^2 coverslips. At 40-50% confluency, they were exposed to a designated concentration of Fe_3O_4-DPA-PEG-FA/FITC NPs (5 µg/mL) for 1 h at 37 °C in the CO_2 incubator. Fixation involved washing the cells (3×) with PBS, followed by 10 min incubation with 2% formaldehyde in PBS at room temperature. After washing cells (3×) with PBS, they were mounted on slides using mounting medium without/with DAPI (50 µM, for 20 min) for nuclear staining. The prepared samples were examined utilizing an Olympus IX81 compound fluorescence microscope equipped with XM10 monochrome camera, Olympus optical Co., Ltd. (Tokyo, Japan) as described previously.

Cellular Impacts

To pursue the cellular impacts of the targeted fluorophoromagnetic nanoparticles, MTT cytotoxicity assay was used. The cultivated cells, at 40-50% confluency, were exposed to Fe_3O_4-DPA-PEG-FA/FITC NPs (0-5 µg/mL). The media was removed and 150 µL fresh media plus 50 µL MTT solutions (prepared as 2 mg/mL in FBS) were added to each well and incubated for 4 h at 37 °C in a CO_2 incubator. The media was removed and the cells were washed (3×), then the formed formazin crystals were dissolved by adding DMSO (200 µL) and Sorenson's buffer (25 µL) to each well plate. The absorbance was read at 570 nm using a spectrophotometer (BioTek Instruments, Inc., Bad Friedrichshall, Germany).

Results

Characterization of Fe_3O_4 Nanoparticles

The synthesized Fe_3O_4 nanoparticles at 270°C by thermal decomposition reaction of Fe $(acac)_3$ showed average size about 7 nm (Figure 1, step 1). For removal of water from reaction environment, the reaction mixture was performed using Dean-Stark apparatus at 120 °C. Size of Fe_3O_4 MNPs was determined using a particle size analyser Zetasizer Nano ZS (Malvern Instruments, UK). As shown in Figure 2A, the surface modification of MNPs with oleylamine layer analysed by FT-IR spectroscopy that revealed the main absorption peaks for oleylamineare: ν (NH_2) 3435 cm^{-1}, ν_{max}/cm^{-1} 3001(=C-H) and 2954s, 2924s, 2852s (C-H); and the explicit absorption peaks related to Fe_3O_4 are: ν_{max}/cm^{-1} 630, 588, 442(Fe-O). Figure 2A shows another important peak at 1523 that represents coordinated bond between Fe (III) of Fe_3O_4 and NH_2 of oleylamine (Fe-N bond).

Characterization of DPA-PEG-NH_2

For synthesis of DPA-PEG-NH_2, in the first step BBrAC-PEG was synthesized by reacting excess amount of bromoacetyl chloride with PEG in the presence of triethylamine as a base. The FT-IR spectroscopy (Figure 2) validated formation of the BBrAC-PEG, resulting in ν_{max}/cm^{-1} 1750 (C=O, PEG-bromoacetyl), 1100 (C-O-C, PEG) and 2880s (CH_2). The peak at 1750 cm^{-1} confirms existence of

carboxylate in structure of PEG. In the second step, reaction of BBrAC-PEG with one equivalent of dopamine yielded DPA-PEG-BrAc. FT-IR spectrum confirmed existence of phenyl ring in DPA-PEG-BrAcwith ν_{max}/cm^{-1} 3100s(=C-H). In the third step, the DPA-PEG-BrAc was treated with N-tert-butoxycarbonyl-1,2-ethylenediamineto gain DPA-PEG-NHBoc, in which the boc (N-tert-butoxycarbonyl) was removed by trifluoroacetic acid (TFA). The synthesis of DPA-PEG-NH_2 was also confirmed by H-NMR.

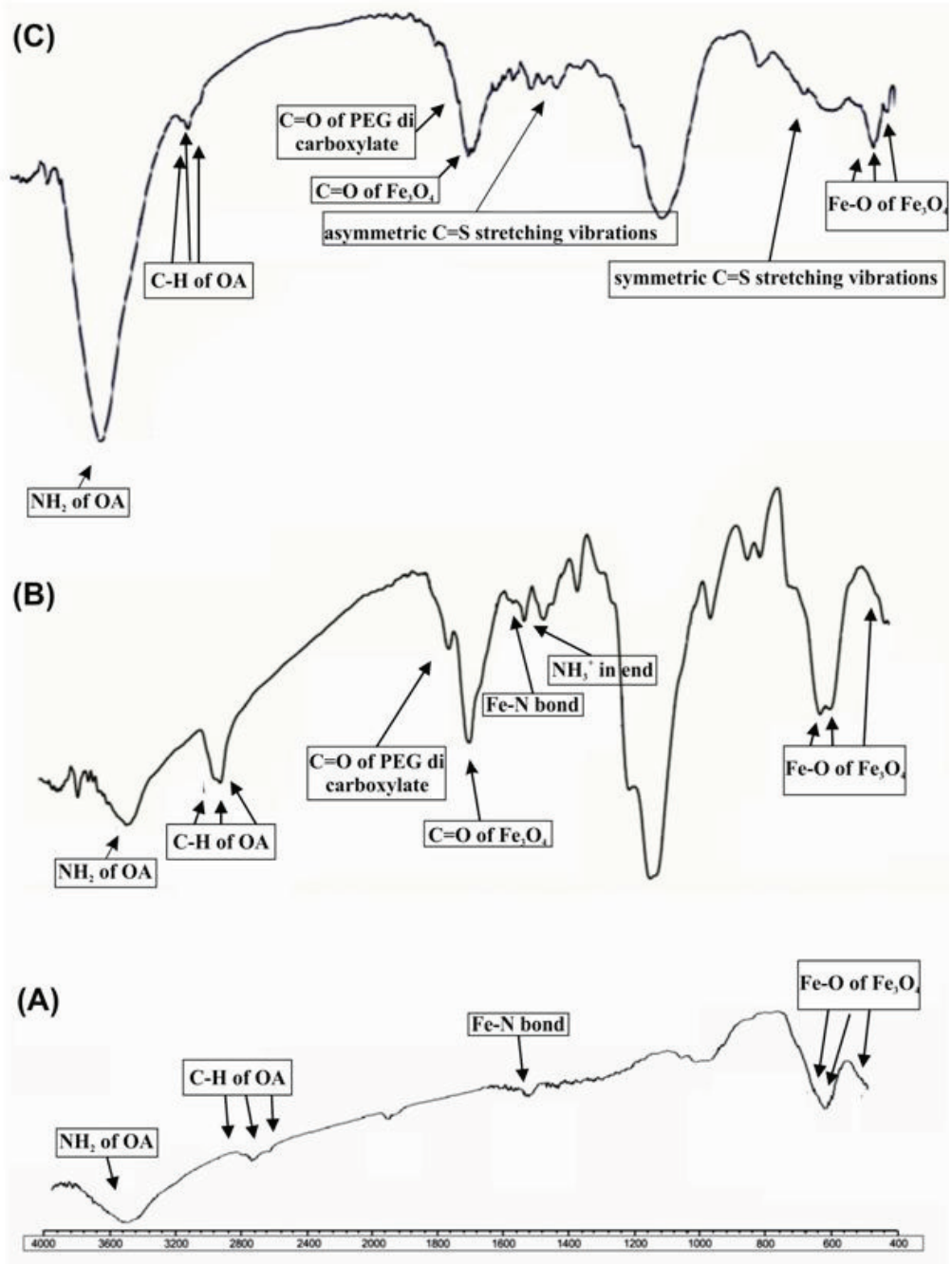

Figure 2. FT-IR spectrophotometer of synthesized Fe_3O_4-DPA-PEG-FA/FITC nanoparticles. A) Fe_3O_4- MNPs. B) Fe_3O_4-DPA-PEG-NH_2, absorption peak in v (1487 cm-1) is related to NH_3^+ available in salt of NH_2TFA. C) Fe_3O_4-DPA-PEG-FA/FITC, the symmetric and asymmetric C=S stretching vibrations at 730 and 1417 cm^{-1} confirmed the formation of thiourea group in the Fe_3O_4- DPA-PEG-FA/FITC.

Characterization of Modified Fe_3O_4

The surface of Fe_3O_4 was modified with DPA-PEG-NH_2 using dopamine moiety. Dopamine has been used as an anchoring agent in DPA-PEG-NH_2 that could replace the oleylamine on surface of Fe_3O_4 MNPs. TEM and SEM micrographs determined the morphology and size of Fe_3O_4-DPA-PEG-NH_2 with diameter ~13 nm (data not shown). In the FT-IR spectrum of the Fe_3O_4-DPA-PEG-NH_2, in addition to the peaks related to Fe_3O_4 and DPA-PEG, absorption peak at ν_{max}/cm^{-1}1487 cm^{-1} is seen that is related to NH_3^+ available in salt of NH_2TFA at the end of the

structure of the Fe_3O_4-DPA-PEG-NH_2 (Figure 2B). To quantify the exact amount of the DPA-PEG-NH_2 used to coat the Fe_3O_4 cores, the solvent media of the supernatant was removed using rotary evaporator and the remained DPA-PEG-NH_2 was analyzed.

Characterization of Fluorophor Conjugated-Fe_3O_4 Magnetic Nanoparticles

When half equivalent FITC and half equivalent FA were conjugated to one equivalent of Fe_3O_4-DPA-PEG-NH_2, both moieties (i.e., FA and FITC) were available on FA and FITC grafted MNPs. FA was used to target the FR, while FITC was used to provide a possibility for fluorescence microscopy of cancer cells. FT-IR analysis of FA-MNPs-FITC confirmed conjugation of FITC onto the MNPs (Figure 2C). The symmetric and asymmetric C=S stretching vibrations at 730 and 1417 cm^{-1} confirmed the formation of thiourea group in the Fe_3O_4-MNP-FA/FITC. Furthermore, bond at 3435 cm^{-1} related to NH_2 stretching was detected on surface of MNPs. The TEM and SEM determined the morphology and size (~30 nm) of Fe_3O_4-DPA-PEG-FA/FITC (Figure 3).

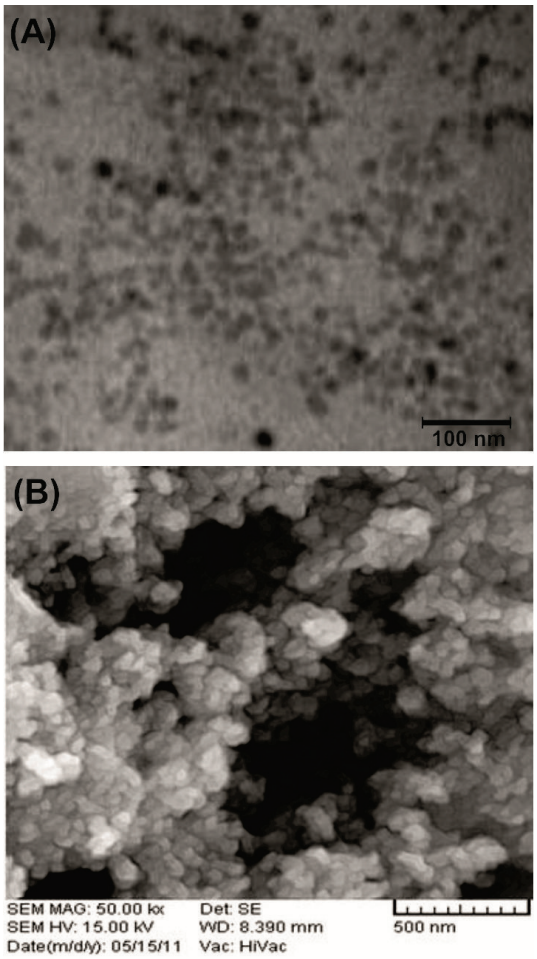

Figure 3. TEM (A) and SEM (B) nano-graph Fe3O4-DPA-PEG-FA/FITC nanoparticles. TEM: transmission electron microscopy. SEM: scanning electron microscopy.

Fluorescence Microscopy and Cellular Impacts

To visualize the cellular interaction of the FR targeted fluoromagnetic NPs, the FR-positive MCF-7 cells and the FR-negative A549 cells were exposed to Fe_3O_4-DPA-PEG-FA/FITC (5 µg/mL) for 1 h. Figure 4 represents the fluorescence microscopy of the MCF-7 cells treated with FR targeted fluoromagnetic NPs. We witnessed substantial binding and/or internalization of the FR targeted fluoromagnetic NPs in the FR-positive MCF-7 cells (Figure 4), but not the FR-negative A549 cells (data not shown), indicating the specificity of these nanosystems toward folate receptor expressing cells.

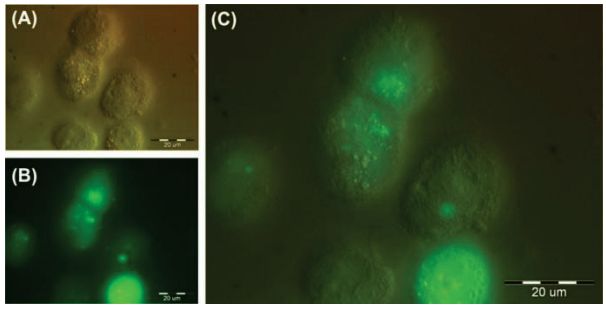

Figure 4. Fluorescence and light microscopy of the MCF-7 cells treated with Fe_3O_4-DPA-PEG-FA/FITC. A) Differential interference contrast (DIC) microscopy image of the MCF-7 cells. B) Fluorescence microscopy (FM) image of the MCF-7 cells treated with fluorophore tagged nanoparticles (MNPs-FA/FITC).C) Superimposed DIC and FM image.

Since these FR targeting fluoromagnetic NPs are used for targeted imaging, we aimed to see their nonspecific toxicity using MTT assay. Figure 5 represents the viability of the treated MCF-7 cells with designated amount of FR targeting fluoromagnetic NPs, which indicate negligible cytotoxicity.

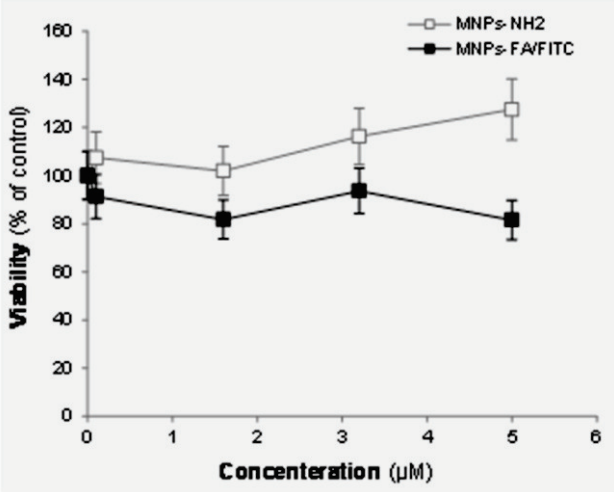

Figure 5. Cellular impacts of Fe_3O_4-DPA-PEG-FA/FITC in MCF-7 cells.

Discussion

Given the fact that nanosized macromolecules are often prone to opsonisation by MPS, the MNPs are PEGylated to become stealth. Such modified MNPs

appear to show markedly long circulation in blood and thus high level of extravasation and accumulation in the tumor site. They were seen as clustered inside the various stages of endocytic pathways without damaging cellular organelles where endocytosis mechanism for their entry appears to be a receptor mediated endocytosis,[26] mainly through targeting a CMM such as FR. It should be noted that the absorption of folate is primarily mediated by a membrane transporter with micro-molar affinities for folates, in which the FRs with nanomolar affinities to folate are likely to markedly modulate folate availability for these transporters and functional isoforms of FRs are anchored to the membrane by a glycolipid anchor, the glycosylphosphatidylinositol (GPI) anchor.[27] Further, colocalization of folate and transferrin receptors[28] clearly indicate that the endocytosis of the targeted fluoromagnetic NPs is a receptor mediated process, presumably via calthrin coated pites and/or membranous caveolae. Thus, we aimed to look at the internalization of FR targeting fluoromagnetic NPs in FR-expressing cells.

We synthesized Fe_3O_4 NPs by thermal decomposition reaction of $Fe(acac)_3$ and undertook a series of surface modification steps to achieve FITC and FA conjugated MNPs (Figures 1-3). The synthesized Fe_3O_4 NPs through thermal decomposition reaction of $Fe(acac)_3$ showed average size about 10 nm, similar to previous reports.[22] We used the DPA-PEG-NH_2 to coat the Fe_3O_4 NPs to achieve more hydrophilic and stealth MNPs. Further, the DPA-PEG-NH_2 modification can provide a versatile platform for further conjugation of MNPs with other functional groups.[29] The PEGylated MNPs (Fe_3O_4-DPA-PEG-NH_2) were conjugated with FA and FITC to produce Fe_3O_4-DPA-PEG-FA/FITC NPs. We used FA to actively target the FR, at which these FA armed MNPs can specifically target the FR-positive breast cancer cells.[30]

Our fluorescence microscopy analysis resulted in significant uptake of FR targeting fluoromagnetic NPs by the FR-positive MCF-7 cells (Figure 4). The time-dependency of this process indicate the binding of the MNPs to the cell surface via folate receptor and endocytosis via vesicular trafficking. Following cellular uptake, membrane-encapsulated silicon particles migrated to the perinuclear region of the cell by a microtubule-driven mechanism.[31] Based upon our flow cytometry analysis, the FR targeting MNPs appeared to specifically quantitatively (>95%) detect the FR expressing cells,[18] while no specific cytotoxicity was observed in the treated cells even with high concentration of FR targeting fluoromagnetic NPs (Figure 5). We speculate that they harness the vesicular trafficking pathway(s) for internalization, i.e. the early/late endosomal machineries. Thus, these nanocarriers, if used as drug delivery nanosystem, should be able to escape from demise in the late endsome/lysosome. Lysosomes contain approximately over 40 different hydrolytic enzymes that mediate controlled intracellular degradation of macromolecules.[32] Thus, due to uniqueness of these trafficking machineries (enzyme composition and pH), targeted MNPs grafted with cytotoxic agents should be engineered in a way to be able to exploit such potential. These FR targeting fluoromagnetic NPs, however, prior to transformation into clinical application, should be fully characterized and tested in appropriate animal models.

Conclusion

The nano-scaled targeted fluoromagnetic theranostics have great potential toward simultaneous imaging and therapy. In this work, we have demonstrated successful synthesis of folic acid/ fluorescein isothiocyanate-PEG conjugated magnetic nanoparticles which could markedly detect the FR expressing cancer cells. Thus, we propose that they can be quantitatively used for specific MRI-based imaging and therapy of various cancers.

Acknowledgments

Authors are thankful to the Research Centre for Pharmaceutical Nanotechnology (RCPN) at Tabriz University of Medical Sciences for the financial support.

Conflict of Interest

The authors declare there is no Conflict of interest in the content of this study.

References

1. Omidi Y. Smart multifunctional theranostics: Simultaneous diagnosis and therapy of cancer. *BioImpacts* 2011;1(3):145-7.
2. Lee N, Hyeon T. Designed synthesis of uniformly sized iron oxide nanoparticles for efficient magnetic resonance imaging contrast agents. *Chem Soc Rev* 2012;41(7):2575-89.
3. Bu L, Xie J, Chen K, Huang J, Aguilar ZP, Wang A, et al. Assessment and comparison of magnetic nanoparticles as mri contrast agents in a rodent model of human hepatocellular carcinoma. *Contrast Media Mol Imaging* 2012;7(4):363-72.
4. Corr SA, Byrne SJ, Tekoriute R, Meledandri CJ, Brougham DF, Lynch M, et al. Linear assemblies of magnetic nanoparticles as mri contrast agents. *J Am Chem Soc* 2008;130(13):4214-5.
5. Yigit MV, Moore A, Medarova Z. Magnetic nanoparticles for cancer diagnosis and therapy. *Pharm Res* 2012;29(5):1180-8.
6. Tietze R, Lyer S, Durr S, Alexiou C. Nanoparticles for cancer therapy using magnetic forces. *Nanomedicine (Lond)* 2012;7(3):447-57.
7. Li C, Li L, Keates AC. Targeting cancer gene therapy with magnetic nanoparticles. *Oncotarget* 2012;3(4):365-70.
8. Ferrari M. Cancer nanotechnology: Opportunities and challenges. *Nat Rev Cancer* 2005;5(3):161-71.

9. Zhou J, Wu W, Caruntu D, Yu MH, Martin A, Chen JF, et al. Synthesis of porous magnetic hollow silica nanospheres for nanomedicine application. *J Phys Chem C* 2007;111(47):17473-7.
10. Robinson I, Tung Le, Maenosono S, Walti C, Thanh NT. Synthesis of core-shell gold coated magnetic nanoparticles and their interaction with thiolated DNA. *Nanoscale* 2010;2(12): 2624-30.
11. Kohler N, Fryxell GE, Zhang M. A bifunctional poly (ethylene glycol) silane immobilized on metallic oxide-based nanoparticles for conjugation with cell targeting agents. *J Am Chem Soc* 2004;126(23):7206-11.
12. Shubayev VI, Pisanic TR, 2nd, Jin S. Magnetic nanoparticles for theragnostics. *Adv Drug Deliv Rev* 2009;61(6):467-77.
13. Bae KH, Kim YB, Lee Y, Hwang J, Park H, Park TG. Bioinspired synthesis and characterization of gadolinium-labeled magnetite nanoparticles for dual contrast t(1)- and t(2)-weighted magnetic resonance imaging. *Bioconjug Chem* 2010;21(3):505-12.
14. Gupta AK, Gupta M. Synthesis and surface engineering of iron oxide nanoparticles for biomedical applications. *Biomaterials* 2005;26(18):3995-4021.
15. Xie J, Xu C, Kohler N, Hou Y, Sun S. Controlled pegylation of monodisperse Fe_3O_4 nanoparticles for reduced non-specific uptake by macrophage cells. *Adv Mater* 2007;19(20):3163-6.
16. Yoo HS, Park TG. Folate-receptor-targeted delivery of doxorubicin nano-aggregates stabilized by doxorubicin-peg-folate conjugate. *J Control Release* 2004;100(2):247-56.
17. Kohler N, Sun C, Wang J, Zhang M. Methotrexate-modified superparamagnetic nanoparticles and their intracellular uptake into human cancer cells. *Langmuir* 2005;21(19):8858-64.
18. Heidari Majd M, Asgari D, Barar J, Valizadeh H, Kafil V, Coukos G, et al. Specific targeting of cancer cells by multifunctional mitoxantrone conjugated magnetic nanoparticles. *J Drug Target* 2013; in press. doi: 10.3109/1061186X.2012.750325.
19. Hu FX, Neoh KG, Kang ET. Synthesis and in vitro anti-cancer evaluation of tamoxifen-loaded magnetite/plla composite nanoparticles. *Biomaterials* 2006;27(33):5725-33.
20. Akça Ö, Ünak P, Medine Eİ, Özdemir Ç, Sakarya S, Timur S. Fluorescein isothiocyanate labeled, magnetic nanoparticles conjugated D-penicillamine-anti-metadherin and in vitro evaluation on breast cancer cells. *Rev Bras Fisica Med* 2011;5(1):99-104.
21. Zhang J, Rana S, Srivastava RS, Misra RD. On the chemical synthesis and drug delivery response of folate receptor-activated, polyethylene glycol-functionalized magnetite nanoparticles. *Acta Biomater* 2008;4(1):40-8.
22. Wang B, Xu C, Xie J, Yang Z, Sun S. Ph controlled release of chromone from chromone-fe3o4 nanoparticles. *J Am Chem Soc* 2008;130(44):14436-7.
23. Moros M, Pelaz B, Lopez-Larrubia P, Garcia-Martin ML, Grazu V, de la Fuente JM. Engineering biofunctional magnetic nanoparticles for biotechnological applications. *Nanoscale* 2010;2(9):1746-55.
24. Sonvico F, Mornet S, Vasseur S, Dubernet C, Jaillard D, Degrouard J, et al. Folate-conjugated iron oxide nanoparticles for solid tumor targeting as potential specific magnetic hyperthermia mediators: Synthesis, physicochemical characterization, and in vitro experiments. *Bioconjug Chem* 2005;16(5):1181-8.
25. Li M, Selvin PR. Amine-reactive forms of a luminescent diethylenetriaminepentaacetic acid chelate of terbium and europium: Attachment to DNA and energy transfer measurements. *Bioconjug Chem* 1997;8(2):127-32.
26. Kumar M, Singh G, Arora V, Mewar S, Sharma U, Jagannathan NR, et al. Cellular interaction of folic acid conjugated superparamagnetic iron oxide nanoparticles and its use as contrast agent for targeted magnetic imaging of tumor cells. *Int J Nanomedicine* 2012;7:3503-16.
27. Sabharanjak S, Mayor S. Folate receptor endocytosis and trafficking. *Adv Drug Deliv Rev* 2004;56(8):1099-109.
28. Yang J, Chen H, Vlahov IR, Cheng JX, Low PS. Evaluation of disulfide reduction during receptor-mediated endocytosis by using fret imaging. *Proc Natl Acad Sci U S A* 2006;103(37):13872-7.
29. Kang SM, Choi IS, Lee KB, Kim Y. Bioconjugation of poly(poly(ethylene glycol) methacrylate)-coated iron oxide magnetic nanoparticles for magnetic capture of target proteins. *Macromol Res* 2009;17(4):259-64.
30. Li K, Jiang Y, Ding D, Zhang X, Liu Y, Hua J, et al. Folic acid-functionalized two-photon absorbing nanoparticles for targeted mcf-7 cancer cell imaging. *Chem Commun (Camb)* 2011;47(26):7323-5.
31. Ferrati S, Mack A, Chiappini C, Liu X, Bean AJ, Ferrari M, et al. Intracellular trafficking of silicon particles and logic-embedded vectors. *Nanoscale* 2010;2(8):1512-20.
32. Barar J, Omidi Y. Cellular trafficking and subcellular interactions of cationic gene delivery nanomaterials. *J Pharm Nutr Sci* 2011;1(1):68-81.